Journal of Ovonic Research Vol. 11, No. 5, September - October 2015, p. 235 - 241

SYNTHESIS AND RIETVELD WHOLE-PATTERN ANALYSIS OF Sr-DOPED PEROVSKITE BISMUTH FERRITE

A. F. HEGAB[a*], I. S. AHMED FARAG[a], A. M. EL-SHABINY[a],
A. M. NASSAAR[b], A. A. RAMADAN[c]
[a]*X-Ray Lab, Solid State Physics Department, National Research Center, Dokki, Cairo, Egypt*
[b]*Physics Department, Faculty of Science, El-Azhar University, Cairo, Egypt*
[c]*Physics Department, Faculty of Science, Helwan University, Cairo, Egypt*

Doping of perovskite bismuth ferrite ($BiFeO_3$) affect greatly its microstructure characteristics. X-ray diffraction analysis using Reitveld method of the whole-pattern fitting is a very useful approach to study the structure variation in relation to doping level. Phase identification, crystallite size, residual microstrain, lattice parameters and bond lengths have been investigated. The conventional solid state reaction method at 650 and 800 °C for 1 h with intermediate grinding was used for the preparation of a series of $Bi_{1-x}Sr_xFeO_3$ (x = 0.1 - 0.5). FULLPROF program was used and modified THOMPSON Cox-HASTING PESUDO-VOIGT function was applied and the background was modeled with fourth order. The sample of x = 0.1 consists of two polymorphic phases perovskite cubic and rhombohedral, the cubic one as the major phase and the rhombohedral one as the minor one. For samples of x = 0.2 - 0.45, only single phase of cubic perovskite structure was identified while for x = 0.5 the sample consists of cubic perovskite and traces of unidentified phase. A continuous decrease in the lattice parameter as well as in the octahedral and dodechaderal bond lengths was observed with increasing Sr^{2+} content and this may be attributed to the increasing number of oxygen vacancies with increasing doping level. The micostrain was found to increase with increasing the Sr^{2+} content, which was attributed also to the formation of point defects (oxygen vacancies) as well as to ionic size mismatch between host and substituent cations that is led to local structural disorder. The crystallite size increases with increasing the doping level which seems to be due to the increase in the surface free energy resulting in the enhancement of the size growth by the presence of oxygen vacancies.

(Received June 29, 2015; Accepted October 8, 2015)

Keywords: Perovskite bismuth ferrite, Sr-doping, XRD, Whole pattern fitting, Rietveld method

1. Introduction

Multiferroic perovskite $BiFeO_3$ (BFO) [1] materials are interesting due to their fascinating technological applications, such as multistate memory devices, spintronic devices, magnetically modulated transducers, ultrafast optoelectronic devices and sensors [2–5]. However, undoped BFO (ABO_3) exhibits secondary phase as an impurity, which leads to large leakage current and restricts its applications. The formation of secondary phase can be suppressed by proper doping at A or B site or both sites of BFO [6,7]. Thus, the main focus of most studies is on the use of dopants such as rare earth metals, transition metals and alkaline earth metals to achieve a single phase of BFO.

The aliovalent substitution such as Ba^{2+}, Pb^{2+}, Sr^{2+} and Ca^{2+} at bismuth site results in stabilization of low symmetric crystal structure which can improve the megnetoelectric and optical properties of the doped BFO. On the other hand, the doping also generates many controversies in scientific community related to the structural and lattice defect. In most of the studies, Sr^{2+}, Ca^{2+}, Pb^{2+} and Ba^{2+} doped BFO ceramics are indexed with rhombohedral structure [8-11]. Contrary to

these reports, other researchers have claimed the cubic, orthorhombic and triclinic structure for different doped BFO systems [12-14]. Similarly, Pokalitov et al. [15] and Li et al. [16] have reported the cubic structure (Pm-3m) for $0.20 \leq x \leq 0.67$ whereas, Varshenay et al. [17] have reported the tetragonal structure (P4/mmm) of $Bi_{1-x}Sr_xFeO_3$ ($0.1 \leq x \leq 0.25$) system.

The motivation of the present work is to investigate the effect of Sr^{2+} (1.26 Å) of larger size than the parent cation Bi^{3+} (1.17 Å) on the structural characteristics of BFO. XRD technique and full pattern fitting analysis of Rietveld method will be used in the present investigations.

2. Experimental and computational

A series of $Bi_{1-x}Sr_xFeO_3$ (x= 0.1, 0.2, 0.25, 0.3, 0.35, 0.45 and 0.5) were synthesized by conventional solid state reaction method using powders of Bi_2O_3 (99.9%), SrO (99.9%), and Fe_2O_3 (99.8 %) in their stoichiometric ratio. The mixtures were, then, grounded for 3 h and heated at 650 and 800 °C for 1 h with intermediate grinding.

The X-ray powder diffraction data were collected using Panalytical Empyrean diffractometer. The measurements were carried out at room temperature using Ni-filtered Cu Kα radiation (λ = 1.5418 Å) with an accelerating voltage of 45 kV and a current of 30 mA. The patterns were scanned in the 2θ range of 15-80°, with step size of 0.013° in 2θ and time per step of 100s. Annealed quartz sample was used as an external standard material under exactly the same conditions for the investigated samples for determining the zero shift and the instrumental profile.

In order to study the effect of Sr substitution on the $BiFeO_3$ compounds, a structure refinement was carried out applying the whole diffraction pattern fitting of Rietveld method [18] implemented in, FULLPROF program [19]. The experimental profile was fitted by modified THOMPSON Cox-HASTING PESUDO-VOIGT function [20], the background was modeled with fourth order polynomial and the preferred orientation was modeled using March's function [21, 22]. In the first step of the refinement the global parameters (instrumental profile, profile asymmetry, background, and specimen displacement) were refined. In the next step, the structural parameters (atomic coordinates, specimen profile breadth parameter, lattice parameter, overall displacement parameter, preferred orientation) were refined in sequence mode. The site occupancy is kept constant to its stoichiometric value. In the last cycle, when the discrepancy factor Rwp (R-weight patterns) has reached its global minimum value, all the parameters (global and structural) were refined simultaneously.

3. Results and discussion

X-ray diffractograms of $Bi_{1-x}Sr_xFeO_3$, are depicted in Figure (1). They reveals that the sample of x = 0.1 consists of two phases, mainly the cubic perovskite polymorphs phase (ICDD 98-008-0799) and minor one of the rhombohedral perovskite (ICDD 98-001-5299). The rhombohedral R3C structure is obtained by $a^-a^-a^-$ octahedral tilting and off-center ionic displacement along [111]c direction. For x = 0.2 - 0.45, the samples consist of single phase of cubic perovskite structure (ICDD 98-008-0799) while for x = 0.5 the sample consists of cubic perovskite (ICDD 98-008-0799) and traces of unidentified phase.

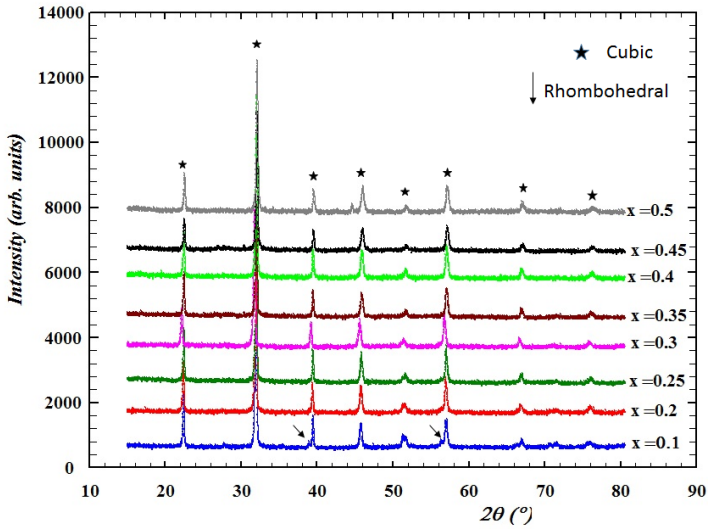

Fig. 1. X-ray diffractograms of $Bi_{1-x}Sr_xFeO_3$

Zooming on in Fig. (2) clearly reveals that as the lower valent cation substitution Sr^{2+} increases ($x \geq 0.2$), the peaks around 2θ = 31-32.5°, which corresponding to the rhombohedral and cubic phases in case of x = 0.1, merge and form a broad peak. The change indicates that rhombohedral structure of $BiFeO_3$ has been modified to higher symmetry phase (cubic phase). This may be due to presence of Sr^{2+} cation that compensating the evaporation of Bi^{3+} cation during the preparation.

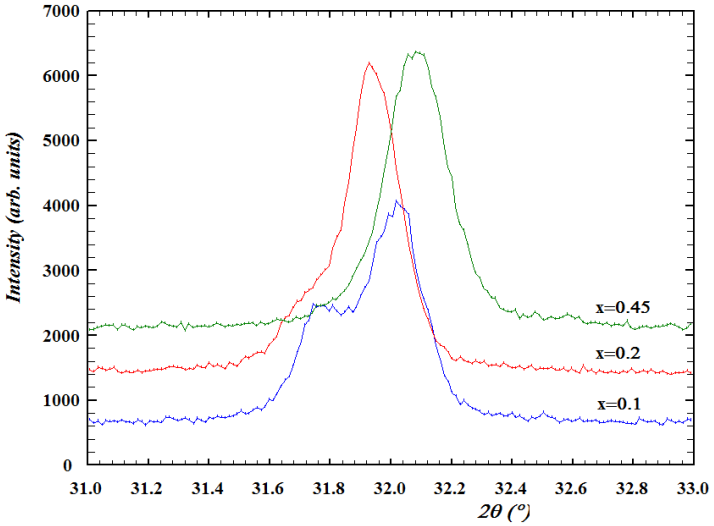

Fig. 2. Zoom in the X-ray diffraction pattern

Several recent reports also showed the transformation to the cubic phase [23 & 24]. Complete structural transformation was observed and in some cases coexistence of two phases has been observed, which solely depends on the ionic radii of the substituted ions and their concentration. Li et al. [23], reported that Sr^{2+} substitution in BFO completely transforms the rhombohedral phase to the cubic phase at x = 0.20. Moreover Bi^{3+} contains $6s^2$ lone pair electrons (Bi: $[Xe]4f^{14}5d^{10}6s^26p^3$). The presence of this highly polarized lone electron pair in $BiFeO_3$ is responsible for the displacement of Bi^{3+} from its centrosymmetric position, causing the formation of rhombohedral structure with the space group R-3c. In the presence of Sr^{2+}, this polar displacement can be suppressed by the formation of oxygen vacancies whereby the lone pair

electron is directed into the empty space of the vacancies. This results in the formation of a more symmetric environment around Bi^{3+} leading to cubic structure.

A comparison of (100) diffraction peak shown in Fig.(2) reveals that for the doped samples, the peak shifts towards the higher diffraction angle with increasing the Sr content. However, these peaks should shift towards lower angle due to the larger ionic radii of Sr^{2+} (1.26 Å) as compared to Bi^{3+} (1.17 Å). The shrinkage of unit cell in the present system makes the hypothesis of formation of oxygen vacancies the most likely and probable.

Reitveld refinement had been done on the single phase sample, i.e (with Sr concentration 0.2 - 0.45). The space group was Pm-3m in which the oxygen anions occupy the Wyckoff position 3c, with coordinates 0; 1/2; 1/2, while the Bi and Sr cations occupy the A-site at Wyckoff position 1a, with coordinates 0; 0; 0, and Fe cation occupy the octahedral site Wyckoff position 1b, with coordinates 1/2; 1/2; 1/2. The agreement between the observed and the calculated diffraction profiles of the sample with x = 0.35 and 0.45 as representative example of the investigated compounds are shown in Fig. (3). the goodness of fit indices are given in Table (1). Their values indicate reliable refined structural parameters.

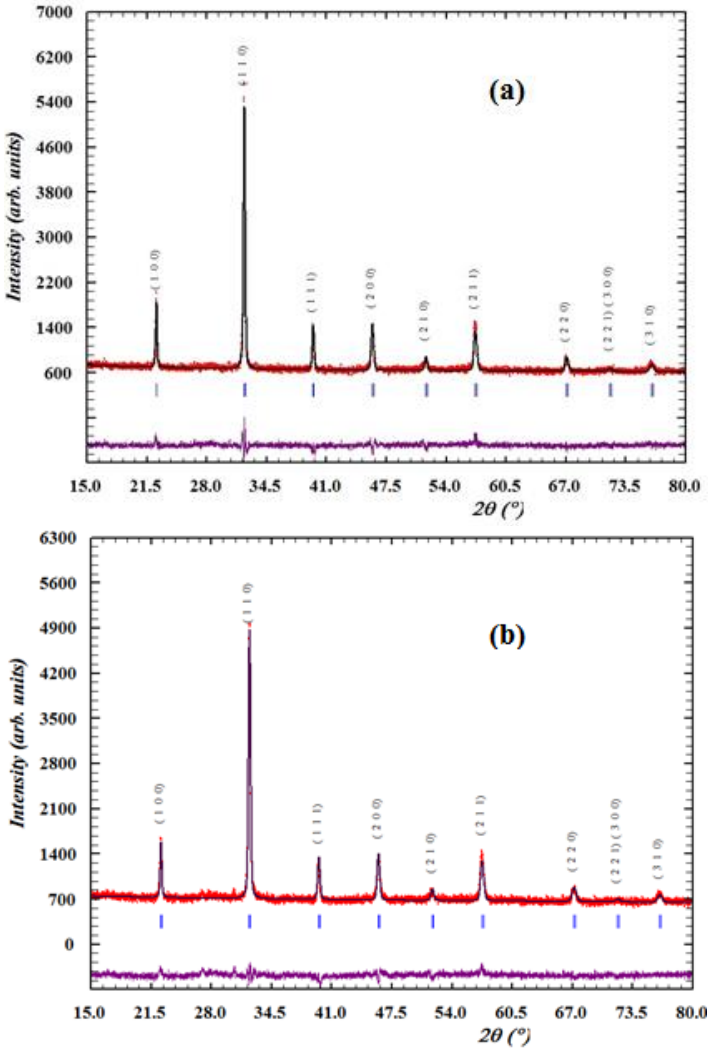

Fig. 3. The observed pattern (circle), the best Rietveld fit profiles (line) and the difference curve between the observed and the calculated profiles (below). for the $Bi_{1-x}Sr_xO_3$: a) x = 0.35 and b) x = 0.45.

Table 1. The goodness of fit indices as well as refined values of the lattice parameter, unit cell volume, strain% overall temperature factor, and bond lengths of the $Bi_{1-x}Sr_xO_3$.

Criteria of fit and structure parameters	Sr concentration (x)					
	0.2	0.25	0.3	0.35	0.4	0.45
R_{wp}	28.2	27.0	25.2	25.6	23.0	26.4
R_p	56.1	51.9	53.7	55.7	52.0	60.8
Chi^2	2.08	1.951	1.509	1.584	1.430	1.514
a (Å)	3.9508	3.9468	3.9462(1)	3.9451	3.9431	3.9405
Cell volume ($Å^3$)	61.667(1)	61.480(2)	61.453(3)	61.399(1)	61.309(1)	61.185(2)
Strain (%)	0.532(5)	0.841(6)	0.925(7)	0.755(5)	0.885(6)	0.958(7)
Overall thermal displacement factor	3.24(4)	3.43(4)	3.018(4)	3.72(4)	3.51(4)	3.58(5)
Fe-O (Å)	1.9738(4)	1.9734(3)	1.9731(1)	1.9725(3)	1.9716(2)	1.9702 (4)
(Bi/Sr)-O (Å)	2.7914(4)	2.7908(3)	2.7904(7)	2.7896(3)	2.7882(3)	2.78633(4)

The refined values of the lattice parameter, the unit cell volume, and the bond lengths of the $Bi_{1-x}Sr_xO_3$ ($0.2<x<0.45$) are given in Table (1). The variation of the refined lattice parameter, a, with Sr-subistution concentration is shown in Fig. (4). A continuous decrease in the lattice parameter was observed with increasing Sr^{2+} content (x). This decrease is due to the increase formation of oxygen vacancies that are created with the Sr substitution due to the charge imbalance. As Sr^{+2} concentration increases the number of generated oxygen vacancies increase which reducing the unit cell dimension. Also, from the values of octahedral and dodechaderal bond lengths given in Table (1), it is clear that, they decrease with increasing the Sr^{2+} substitution and this may be also due to increasing number of oxygen vacancies with increasing doping level.

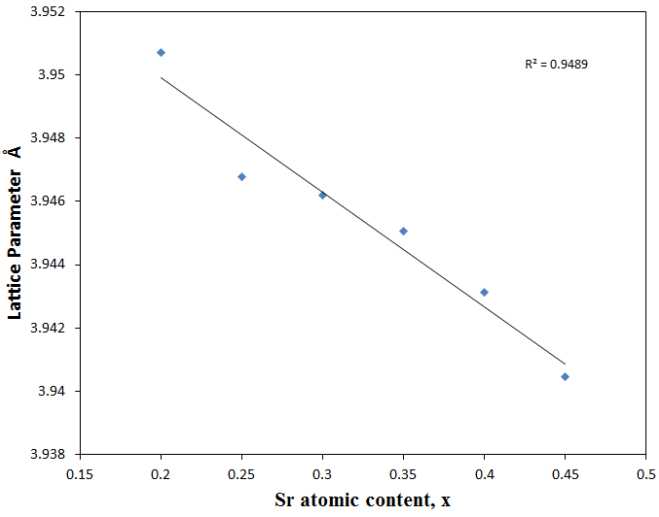

Fig. 4. Relation between the lattice parameters versus Sr atomic content

The micostrain values (Table 1) was found to increase with increasing the Sr^{2+} content. This is attributed to the increase of point defects (oxygen vacancies), which increases with increasing the substituted cation (Sr^{2+}) in addition to ionic size mismatch between host and substituent cations that is lead to local structural disorder. On the other hand, the crystallite size increases with increasing the doping level as depicted in Figure (5). This increase in crystallite size seems to be due to the increase in the surface free energy[25]. As the surface free energy increases, the surface to the volume ratio must be decreases and this will leads to an increase in the crystallite size. In addition, dopant with an oxidation state below 3+ on BFO will increase the oxygen vacancy that leads to enhance the crystallite size growth and the oxygen diffusion would be the rate-controlling step.

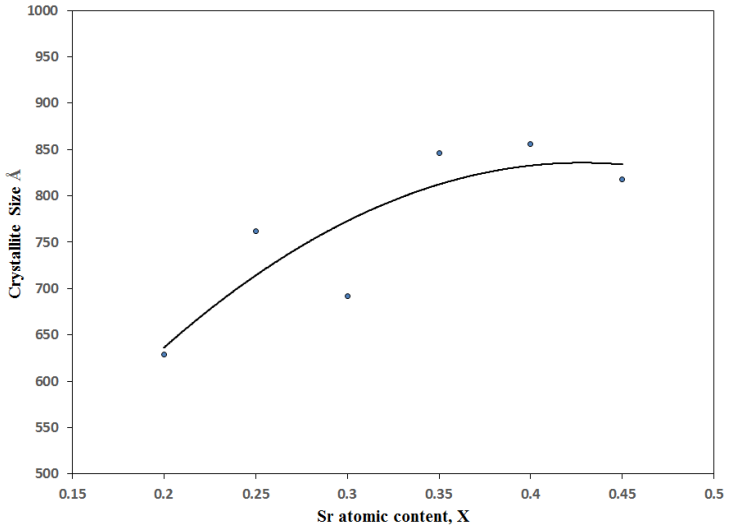

Fig. 5. Variation of the crystallite size with the doping level

4. Conclusions

Sr doping level of perovskite bismuth ferrite affects phases formed by solid state reaction method. Formation of single phase of cubic perovskite depends on the doping concentration of $Bi_{1-x}Sr_xO_3$. The optimum concentration is $0.2> x < 0.45$, lower or higher values result in two phases. As Sr^{+2} concentration increases the number of generated oxygen vacancies increase, which reducing the unit cell dimension as well as the values of octahedral and dodechaderal bond lengths. The internal residual microstrain values increase with increasing the Sr^{2+} content, which is attributed to the formation of oxygen vacancies (point defects) in addition to the effect of the ionic size mismatch between host and substituent cations that is lead to local structural disorder. On the other hand, the crystallite size increases with increasing the doping level due to the increase in the surface free energy and the oxygen vacancy.

References

[1] G. Catalan, J. F. Scott, Adv. Mater. 21, 2463 (2009).
[2] S. W. Cheong, M. Mostovoy, Nat. Mater. 6, 13 (2007).
[3] R. Ramesh, N. A. Spaldin, Nat. Mater. 6, 21 (2007).
[4] A. Singh,V. Pandey, R. K. Kotnala, D. Pandey, Phys. Rev. Lett. 101, 247602 (2008).
[5] J. Wang, J. B. Neaton, H. Zheng, V. Nagarajan, S. B. Ogale, B. Liu, D. Viehland, V. Vaithyanathan, D. G. Schlom, U. V. Waghmare, N. A. Spaldin, K. M. Rabe, M. Wuttig, R.Ramesh, Science, 299, 1719 (2003).
[6] A. Gautam, K. Singh, K. Sen, R. K. Kotnala, M. Singh, Mat. Lett., 65**,** 591 (2011).

[7] X. Zheng, Q. Xu, Z. Wen, X. Lang, D. Wu, T. Qiu, M.X. Xu, J. alloys and comp. 499**,** 108 (2010).
[8] V. A. Khomchenko, D. A. Kiselev, J. M. Vieira, Li Jian, A. L. Kholkin, A. M. L. Lopes, Y. G. Pogorelov, J. P. Araujo, M. Maglione, J. Appl. Phys., 103, 024105 (2008).
[9] V. A. Khomchenko, D. A. Kiselev, J. M. Vieira, A. L. Kholkin, M. A. Sá, Y. G. Pogorelov, Appl. Phys. Lett., 90, 242901 (2007).
[10] P. Li, Y. H. Lin, C. W. Nan, J. Appl. Phys., 110**,** 033922 (2011).
[11] Jaiparkash, Y. Kumar, R.S. Chauhan, R. Kumar, Solid State Sciences, 13, 1869 (2011).
[12] K. Sardar, J. Hong, G. Catalan, P. K. Biswas, M. R. Lees, R. Walton, J. F. Scott S. A. T. Redfern, J. Phys.: Condens. Matter., 24, 045905 (2012).
[13] G. Katopu, A. Lahmar, S. habouti, C. L. Solterbeck, B. Elouadi, M. E. Souni, Appl. Phys. Lett. 92**,** 151910 (2008).
[14] P. Pandit, S. Satapathy, P. K. Gupta, V. G. sathe, J. Appl. Phys., 106, 114105 (2009).
[15] V. V. Pokatilov, V. S. Pokatilov, A. S. Sigov, V. M. Cherepanov, Inorganic Materials, 45, 743 (2009).
[16] J. Li, Y. Duan, H. He, D. Song, J. Alloys and Comp., 315**,** 259 (2001).
[17] D. Varshney, A. Kumar, J. Molecular structure, 1038**,** 241 (2013).
[18] H. M. Rietveld, J. Appl. Cryst., 2, 65 (1969).
[19] J. Rodriguez-Carvajal, Short Reference Guide of the FullProf Progarm, Laboratory Leon Brillouin (CEA-CNRS), version July, (2011).
[20] P. Thomson, D.E. Cox, J.M. Hasting, J. Appl. Crystall., 20, 79 (1987).
[21] A. March, Zeitschrift fur Kristallographie, 81, 285 (1932).
[22] W.A. Dollase, J. Appl Crystall., 19, 267 (1986).
[23] J. Li, Y. Duan, H. He, D. Song, J. Alloys and Compd., 315, 259–64 (2001).
[24] J. Silva, A. Reyes, H. Esparza, H. Camacho, L. Fuentes, Integr. Ferroelectr., 126, 47 (2011).
[25] L. Eckertova, Physics of Thin Films, Plenum Press, New York, P. 306 (1986).